Fiber characterization using confocal microscopy–collapse behavior of mechanical pulp fibers

HO FAN JANG, REZA AMIRI, RAJINDER S. SETH, AND ALKIS KARNIS

ABSTRACT

Confocal laser scanning microscopy (CLSM) was used to measure changes in the transverse dimensions of mechanical pulp fibers produced under different refining conditions. Increasing the specific energy of refining increased the degree of fiber collapse and decreased the fiber cross-sectional area, fiber-wall thickness, and lumen area. The decrease in fiber-wall properties was more pronounced with high-intensity refining, and fiber collapse was further increased by a decrease in fiber-wall rigidity. Fiber properties were also measured by conventional image analysis and surface profilometry techniques. These results agreed with those obtained by the more comprehensive CLSM.

During production of mechanical pulps, energy is consumed in separating the fibers from the wood and in developing their papermaking potential. Fiber properties play an important role in determining pulp and paper quality.

Several works describe the effects of specific energy and refining intensity on pulp properties *(1–5)*. However, very little is known about the effects on development of properties for individual fibers. A mechanism for fiber development in chip refining has recently been proposed *(6)*. This mechanism postulates that the fibers in the refining zone undergo a "peeling-off" action, in which part of the fiber wall is initially delaminated and ultimately detached from the fiber to form short fibers and fines. The extent of fiber delamination and removal of fiber-wall material depends on the amount of applied energy and, possibly, the refining intensity *(6)*. Thus it would be expected that fibers become more collapsible as the specific energy increases. However, no experimental data were provided to substantiate the hypothesis.

Confocal laser scanning microscopy (CLSM) is a powerful new technique for rapidly and nondestructively generating cross-sectional images of wood pulp fibers *(7)*. Combined with image analysis, the CLSM technique can accurately determine fiber transverse dimensions.

The main objective of this work was to use the CLSM technique to determine the effects of specific energy and refining intensity on fiber transverse dimensions and fiber collapse. A second objective was to investigate the reliability of conventional methods *(8)*—image analysis and profilometry—for measuring fiber properties by comparing the results with those obtained by the more accurate CLSM method.

EXPERIMENTAL

Two thermomechanical pulps (TMP) of black spruce and one refiner mechanical pulp (RMP) of 90% black spruce and 10% jack pine were used in this study. The TMP was produced in two stages, with the rotor speed in the first stage set at either 1200 rpm or 1800 rpm. Second-stage rotor speed was kept constant at 1200 rpm. The RMP was produced in a single stage at 1200 rpm. Table I shows the refining conditions for the pulps. Fiber properties were measured on the P14/R28 fraction of a Bauer–McNett fiber-length classifier.

A confocal laser scanning system (Bio-Rad MRC-500), attached to a microscope (Zeiss Axiophot) operated in epifluorescence mode, was used to generate fiber cross-sectional images. All fibers were lightly dyed with fluorochrome dye *(9)*. Samples were prepared by depositing fibers on glass slides, wet pressing them at 350 kPa, and allowing them to air dry *(8)*. During measurements, each fiber was first oriented perpendicular to the laser scanning direction, and an optical section through its thickness was obtained.

Figure 1 shows typical confocal cross-sectional images of TMP fibers obtained with CLSM. Image-analysis techniques were used to measure these images. The details of the CLSM technique and image analysis have been reported elsewhere *(9)*. Figure 2 shows an original confocal image and its processed binary image with the center-line perimeter drawn. Fiber transverse dimensions—cross-sectional area, A; center-line perimeter, P; wall thickness, T ($T = A/P$); fiber thickness, D_{min}; fiber width, D_{max}; lumen area, LA; and aspect ratio ($AR = D_{min}/D_{max}$)—were measured as shown in Fig. 3. The mean values and distributions for the fiber dimensions were calculated from 120 to 180 images of different fibers.

During pulping and papermaking processes, fibers are exposed to external forces that can change their native cross-sectional shape. The

Refining process	First-stage rotational speed, rpm	First-stage intensity, GJ/metric ton per impact	Total specific energy, GJ/metric ton	Freeness of whole pulp, mL CSF
Two-stage TMP[a]				
Low intensity	1200	2.5×10^{-4}	...	...
Sample A5	...	...	8.3	251
Sample A2	...	...	12.4	45
High intensity	1800	3.8×10^{-4}	...	...
Sample A19	...	...	8.4	96
Sample A18	...	...	9.9	57
Single-stage RMP[b]				
Intensity	1200	...	...	...
Sample AK-2	...	...	4.45	253
Sample AK-4	...	...	8.7	43

[a] 100% black spruce; pulps refined first in a pressurized double-disc refiner (Bauer 418), followed by refining in a double-disc open-discharge refiner (Bauer 410) at 1200 rpm
[b] 90% black spruce, 10% jack pine; pulps prepared with a double-disc open-discharge refiner (Bauer 400).

I. Refining conditions

volume or cross-sectional area of the lumen is usually reduced or even eliminated. Such fiber flattening or collapse can be characterized and estimated in different ways *(8, 10, 11)*. For example, lumen area (LA), fiber thickness (D_{min}), and the aspect ratio (D_{min}/D_{max}) in Fig. 3 can indicate the degree of fiber flattening or collapse *(10)*, with smaller LA, D_{min}, and aspect ratio implying a greater degree of collapse. Based on the decrease in fiber-lumen volume or cross-sectional area, we have defined a collapse index (CI) as follows:

$$CI = 1 - (LA/LA_o) \qquad (1)$$

where

LA = lumen area obtained from the cross-sectional image of a fiber (after treatments that may have caused flattening or collapse)

LA_0 = lumen cross-sectional area of the same fiber, as if it had not been subjected to any external forces, and therefore had not collapsed.

LA at any point along the length of a fiber can be measured from its confocal cross-sectional image. LA_0, being unknown, is determined as follows. The native lumen cross-section is assumed to be rectangular, which allows calculation of LA_0 from the measured lumen perimeter and its "estimated" uncollapsed lumen aspect ratio *(12)*. This collapse index is more representative of the collapse behavior of a fiber, as it measures the fractional change in the lumen cross-sectional area with respect to the uncollapsed one. For example, it does not depend on the shape of the collapsed fiber, as does the degree of collapse indicated by D_{min}/D_{max} *(12)*. CI is equal to 1 if a fiber is totally collapsed, whereas it is zero for an uncollapsed fiber. This CI can be used to compare the degree of flattening or collapse for either an individual pulp at increasing levels of treatment or for different pulps. Fiber collapse is an important property because it affects sheet structure and, therefore, the physical properties of the sheet.

Other techniques were also employed to measure the transverse fiber dimensions *(8)*. Fiber coarseness, *C*, was measured by the Clark method, which is based on the principle of statistical geometry of a fiber network *(13)*. Fiber width, *W*, was obtained by measuring the distance between fiber edges of individual fibers deposited on glass slides. Fiber thickness was determined using a stylus profilometer. The deflection of the stylus across the fibers was recorded as fiber thickness. Double fiber-wall thickness, t_{2W}, was computed with the use of the equation developed by Jordan *(14)*:

$$t_{2W} = C/W\rho_{cell} \qquad (2)$$

where

ρ_{cell} = density of the cellulose

A degree of fiber collapse, d, can also be obtained from thickness measurements *(8)*:

$$d = 1 - [(t - t_{2W})/(t_0 - t_{2W})] \qquad (3)$$

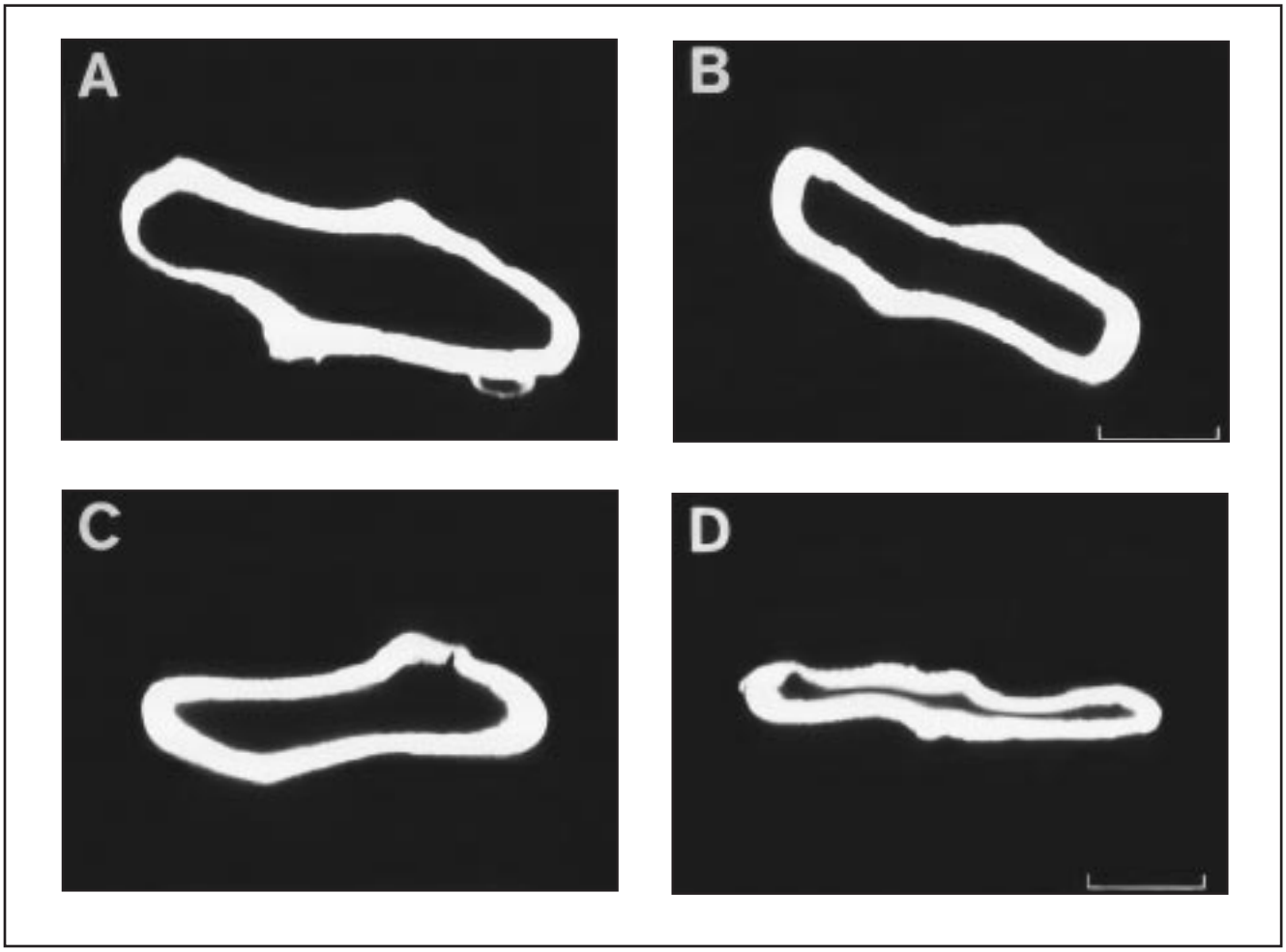

1. Epifluorescence cross-sectional images of air-dried TMP fibers. Fibers in photos a and b were refined at 1200 rpm with specific energies of 8.3 GJ/metric ton and 12.4 GJ/metric ton, respectively. Fibers in photos c and d were refined at 1800 rpm with specific energies of 8.4 GJ/metric ton and 9.9 GJ/metric ton, respectively. Fiber-wall thicknesses in photos a–d were 2.07 µm, 1.91 µm, 1.98 µm, and 1.86 µm, and their respective degrees of collapse were 0.39, 0.43, 0.49, and 0.86.

where

t_0 = thickness of the uncollapsed fiber
t = thickness of the collapsed fiber.

The uncollapsed fiber thickness was estimated assuming that the initial uncollapsed fibers were cylindrical. As Eq. 3 shows, the parameter d indicates the change in fiber thickness rather than the change in lumen area.

RESULTS

Effects of refining

Table II shows the mean values for fiber cross-sectional area, center-line perimeter, and fiber-wall thickness as measured by CLSM. These results show that as the total specific energy increases, the fiber-wall cross-sectional area decreases significantly. For example, the mean cross-sectional area for the fibers of Sample A5 was 144 µm^2 compared with 126 µm^2 for Sample A2. In all cases, however, the different refining conditions had no significant effect on the center-line perimeter. This indicates that the fiber-wall thickness *(T = A/P)* decreases as specific energy increases, in accordance with the peeling-off mechanism proposed earlier *(6)*. That is, as refining proceeds, outer layers of fiber wall are progressively removed and fibers become thinner.

Table III shows the mean values of lumen area, fiber width (D_{max}), fiber thickness (D_{min}), aspect ratio (D_{min}/D_{max}), and collapse index (defined in Eq. 1) obtained from confocal cross-sectional images of fibers. These results show that lumen area, fiber thickness, and

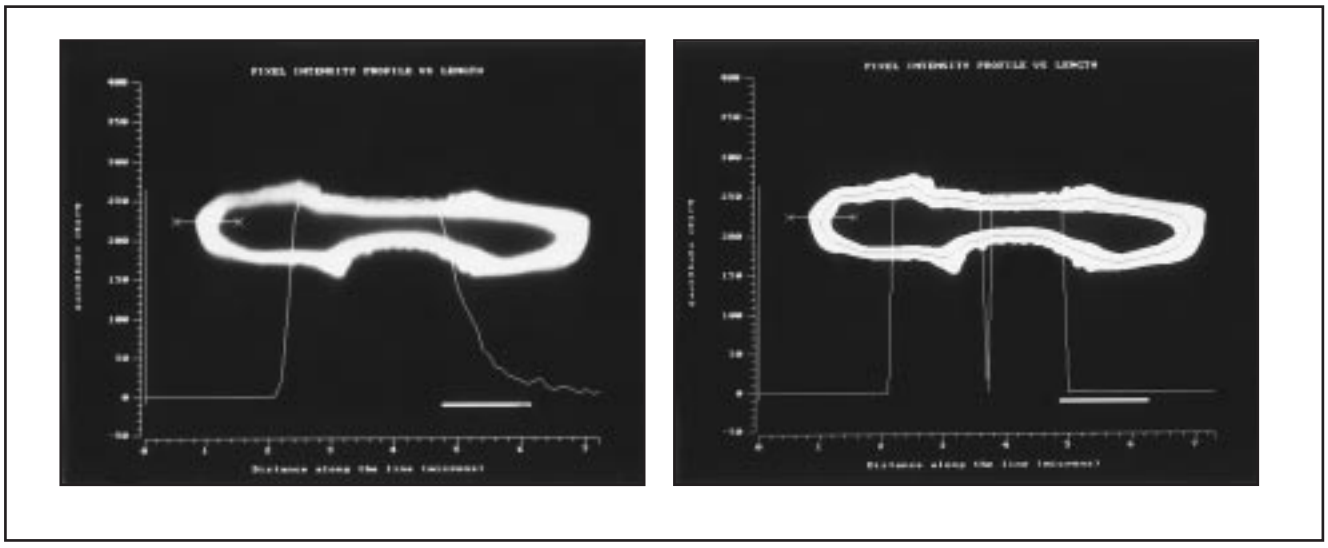

2. Original CLSM image (a) and image after processing (b). The cross-sectional area and center-line perimeter were found to be 200 µm² and 95.9 µm, respectively. Calculated mean wall thickness was 2.10 µm.

aspect ratio decreased with increasing total specific energy. The consequent increase in the collapse index indicates that fibers collapsed more easily at a higher specific energy.

The effects of the specific energy on fiber properties were more pronounced for high-intensity refining than for low-intensity refining, as seen in Fig. 4. Figures 4a and 4b show that both fiber-wall thickness and fiber thickness decreased more rapidly at high refining intensity, while Fig. 4c shows that fiber collapse increased more rapidly at the higher intensity.

Figure 5 shows the collapse index as a function of fiber-wall thickness for the TMPs refined at low intensity (Fig. 5a) and at higher intensity (Fig. 5b). The curves are fits of the data to the function

$$CI = 1 - \exp(-a/T^{ß}) \qquad (4)$$

where a and ß are constants determined by the fit *(12)*.

Both Figs. 5a and 5b show that the degree of fiber collapse increased as the fiber-wall thickness decreased. The propensity of thin-walled fibers to collapse more readily than thick-walled fibers has been shown for chemical pulps *(11)*. For the TMP fibers refined at low intensity but at two levels of specific energy (Fig. 5a), the collapse behavior was similar at a given wall thickness, as indicated by the overlapping of the two curves. However, fibers were, on the average, thinner at the higher specific-energy level and, therefore, more collapsed, as seen in Table III. Indeed, Fig. 5 also shows that, at a given refining intensity,

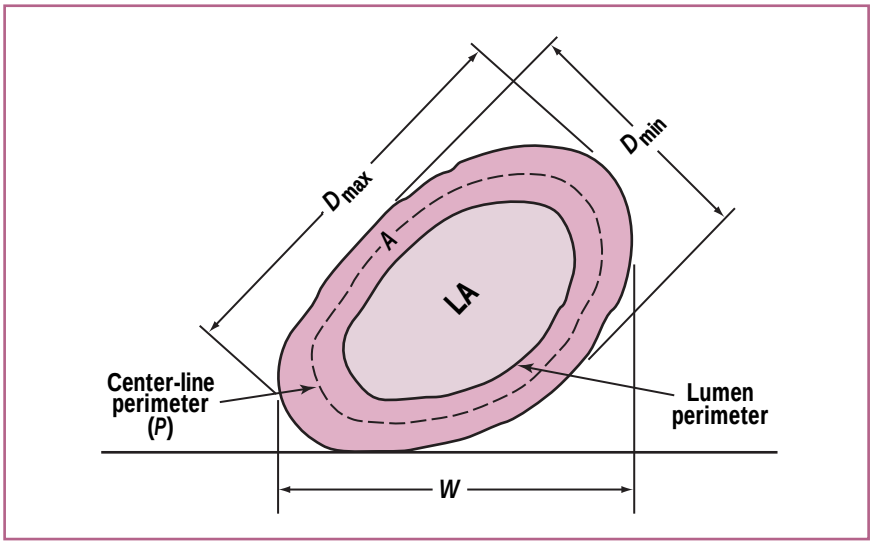

3. After the CLSM image has been processed (e.g., Fig. 2b), the following fiber properties are determined by the image analyzer: **A**, *fiber cross-sectional area;* **LA**, *lumen area;* **P**, *center-line perimeter;* **T**, *mean fiber-wall thickness* (**T = A/P**); D_{max}, *fiber width (longest Feret diameter of fiber);* D_{min}, *fiber thickness (shortest Feret diameter of fiber); aspect ratio (AR =* D_{min}/D_{max}*);* **W**, *projected width.*

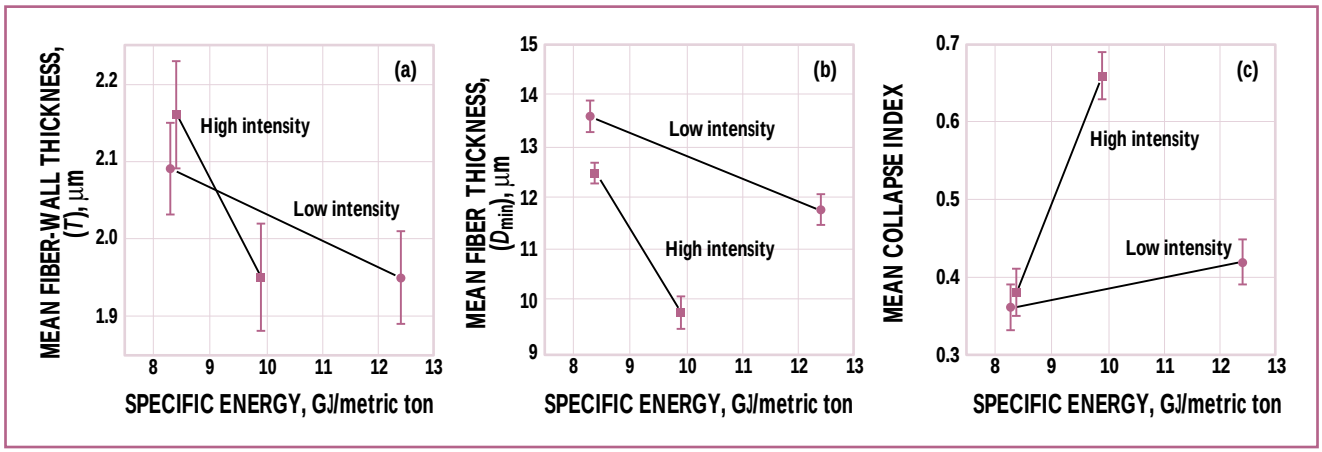

4. Effects of refining intensity on fiber-wall thickness (a), fiber thickness (b), and fiber collapse (c) for TMP

Refining process	Specific energy, GJ/metric ton	Mean cross-sectional area (*A*), m m² ± SD[c]	Mean center-line perimeter (*P*), Em ± SD[c]	Mean wall thickness (*T*), Em ± SD[c]
Two-stage TMP				
Sample A5 (*n*[b] = 179)	8.3	144 ± 4	70.9 ± 1.4	2.09 ± 0.06
Sample A2 (*n* = 179)	12.4	126 ± 3	67.9 ± 1.3	1.95 ± 0.06
Sample A19 (*n* = 143)	8.4	146 ± 4	70.4 ± 1.5	2.16 ± 0.07
Sample A18 (*n* = 128)	9.9	133 ± 4	71.1 ± 1.6	1.95 ± 0.07
Single-stage RMP				
Sample AK-2 (*n*=125)	4.45	169 ± 5	72.3 ± 1.8	2.46 ± 0.08
Sample AK-4 (*n* = 118)	8.7	143 ± 5	70.5 ± 1.8	2.12 ± 0.08

[a] Fiber properties measured on P14/R28 fraction (fibers passing through a 14-mesh screen and retained on a 28-mesh screen) of Bauer McNett fiber-length classifier
[b] *n* = number of fibers
[c] SD = estimated standard deviation of the mean

II. Cross-sectional fiber dimensions as measured with CLSM[a]

there are more thin-walled fibers in pulps refined at higher specific energy. This trend is more apparent in the TMPs refined at high intensity (Fig. 5b).

For fibers refined at high intensity, the relationship between the degree of fiber collapse and fiber-wall thickness was different at the two levels of specific energy, as shown in Fig. 5b. The collapse curve for the low-energy fibers is to the left of that for high energy. Thus at the same wall thickness, fibers refined at high specific energy are more readily collapsed than those at low. This suggests that the elastic modulus of the fiber wall in the transverse plane decreases with increasing specific energy. Fibers tend to collapse more readily when refined to a higher specific energy, probably because of the reduction in the rigidity of fiber-wall material in addition to the decrease in fiber-wall thickness (Fig. 5b). This is supported by the fact that while the mean fiber-wall thickness decreased only moderately for the TMPs refined at high intensity (from 2.16 µm to 1.95 µm, Table II), the mean degree of collapse increased substantially (from 0.38 to 0.66, Table III).

The fiber-wall thickness for TMPs decreased by 0.14 µm and 0.21 µm for low- and high-intensity refining, respectively (Table II). In the latter case, more of the fiber's outer primary wall and, subsequently, the thin outer secondary (S_1) wall would be removed (peeled-off). Removal of the primary wall and the S_1 layer reduces the constraints of the remaining layers, thus promoting internal delamination, which would decrease the rigidity of the fiber.

Refining process	Specific energy, GJ/metric ton	Mean lumen area (LA), μm² ± SD[b]	Mean fiber width (D_{max}), μm ± SD[b]	Mean fiber thickness (D_{min}), μm ± SD[b]	Mean aspect ratio (D_{min}/D_{max}), (dimensionless) ± SD[b]	Mean collapse index (CI), (dimensionless) ± SD[b]
Two-stage TMP						
Sample A5	8.3	139 ± 7	32.3 ± 0.6	13.6 ± 0.3	0.45 ± 0.01	0.36 ± 0.03
Sample A2	12.4	111 ± 6	31.2 ± 0.6	11.8 ± 0.3	0.41 ± 0.01	0.42 ± 0.03
Sample A19	8.4	131 ± 7	33.5 ± 0.7	12.5 ± 0.2	0.40 ± 0.01	0.38 ± 0.03
Sample A18	9.9	69 ± 7	33.6 ± 0.8	9.8 ± 0.3	0.32 ± 0.01	0.66 ± 0.03
Single-stage RMP						
Sample AK-2	4.45	124 ± 7	34.5 ± 0.9	12.8 ± 0.2	0.40 ± 0.01	0.43 ± 0.03
Sample AK-4	8.7	99 ± 8	33.1 ± 0.8	11.1 ± 0.3	0.35 ± 0.01	0.53 ± 0.03

[a] Fiber properties measured on P14/R28 fraction of Bauer McNett fiber-length classifier
[b] SD = estimated standard deviation of the mean

III. Lumen area, fiber width, fiber thickness, aspect ratio, and collapse index obtained from the fiber cross-sectional images as measured by CLSM[a]

The effect of refining intensity on fiber collapse is apparent in Fig. 4c. At low-specific-energy refining, intensity does not appear to affect fiber collapse. However, as the specific-energy level increases above 8 GJ/metric ton, the effect of refining intensity becomes apparent. This is in agreement with previously reported results that high-intensity refining produces fibers of lower coarseness than does low-intensity refining *(6)*.

Comparison of CLSM and conventional measurement of fiber properties

Figure 6 contains six plots of fiber properties as measured by conventional measuring techniques and by CLSM. Figure 6a shows the fiber coarseness obtained by Clark's method vs. the cross-sectional area by CLSM. The fiber coarseness is related to the cross-sectional area by the density of wall material, r_{cell}. From the slope of the best-fit line through the origin in Fig. 6a, the density, r_{cell}, was found to be 1.52 ± 0.04 g/cm³, which is in reasonable agreement with the accepted value of 1.55 g/cm³.

The fiber-wall thickness obtained from Eq. 2 seems to be in agreement with that obtained from CLSM, except for RMP, as seen in Fig. 6b. Note that Eq. 2 tends to overestimate the wall thickness for an uncollapsed fiber *(8)*, since the fiber width *(W)*—the distance measured between the edges of the fiber—would be smaller for an uncollapsed fiber than for a fully collapsed fiber. Nevertheless, both methods showed that fiber-wall thickness decreased with increasing refining energy.

Fiber width as measured with CLSM is higher than that obtained with image analysis, as shown in Fig. 6c. This difference is due to the fact that in CLSM, fiber width is defined as the longest Feret diameter (D_{max} in Fig. 3), whereas in image analysis, fiber width is measured from the projected image of the fiber (*W* in Fig. 3). The projected width is expected to be smaller than D_{max}.

Figure 6d shows D_{min} of the fiber cross-sectional images vs. fiber thickness as measured by profilometry. The D_{min} measurements were larger than the average fiber thickness obtained with the profilometer. This result can be ascribed to two factors. First, D_{min}—defined as the shortest Feret diameter—measures the thickest part of fiber. Second, pressure applied by the profilometer stylus can deform the fiber, thus reducing the measured thickness.

Aspect ratio, defined in CLSM as D_{min}/D_{max}, was larger than the aspect ratio obtained by conventional measurement with a profilometer, as seen in Fig. 6e. The difference was mainly because of the different measurements of fiber thickness obtained using CLSM and profilometry. Nevertheless, both methods confirmed that fiber thickness and aspect ratio decreased with increasing specific energy.

The collapse index associated with fiber thickness (Eq. 3) was higher than that obtained by CLSM, as seen in Fig. 6f. The higher collapse index for the conventional method is directly related to the underlying assumption that untreated fibers are cylindrical. Such an approach overestimates the initial fiber thickness, thus inflating the calculated degree of fiber collapse *(8)*. Still, both methods show that the degree of collapse increased with increasing specific energy.

CONCLUSIONS

Confocal laser scanning microscopy (CLSM) was used to measure the

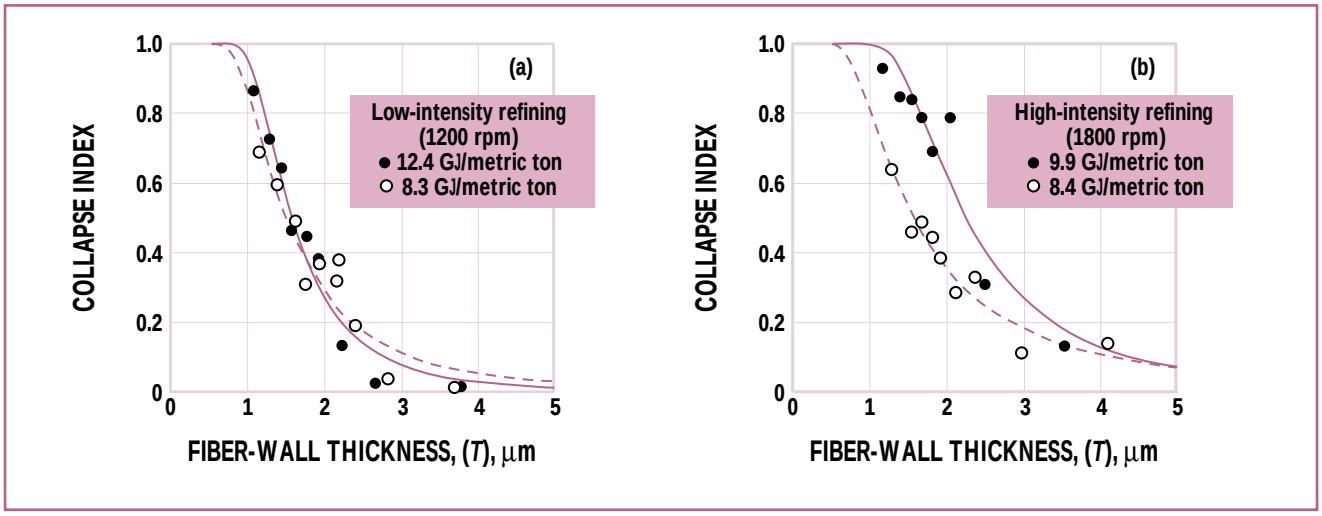

5. Collapse index vs. fiber-wall thickness at two levels of specific energy for TMP at low (a) and high (b) refining intensities. Each point in Fig. 5a represents an average value of 20 fibers. Each point in Fig. 5b represents an average value of 16 fibers.

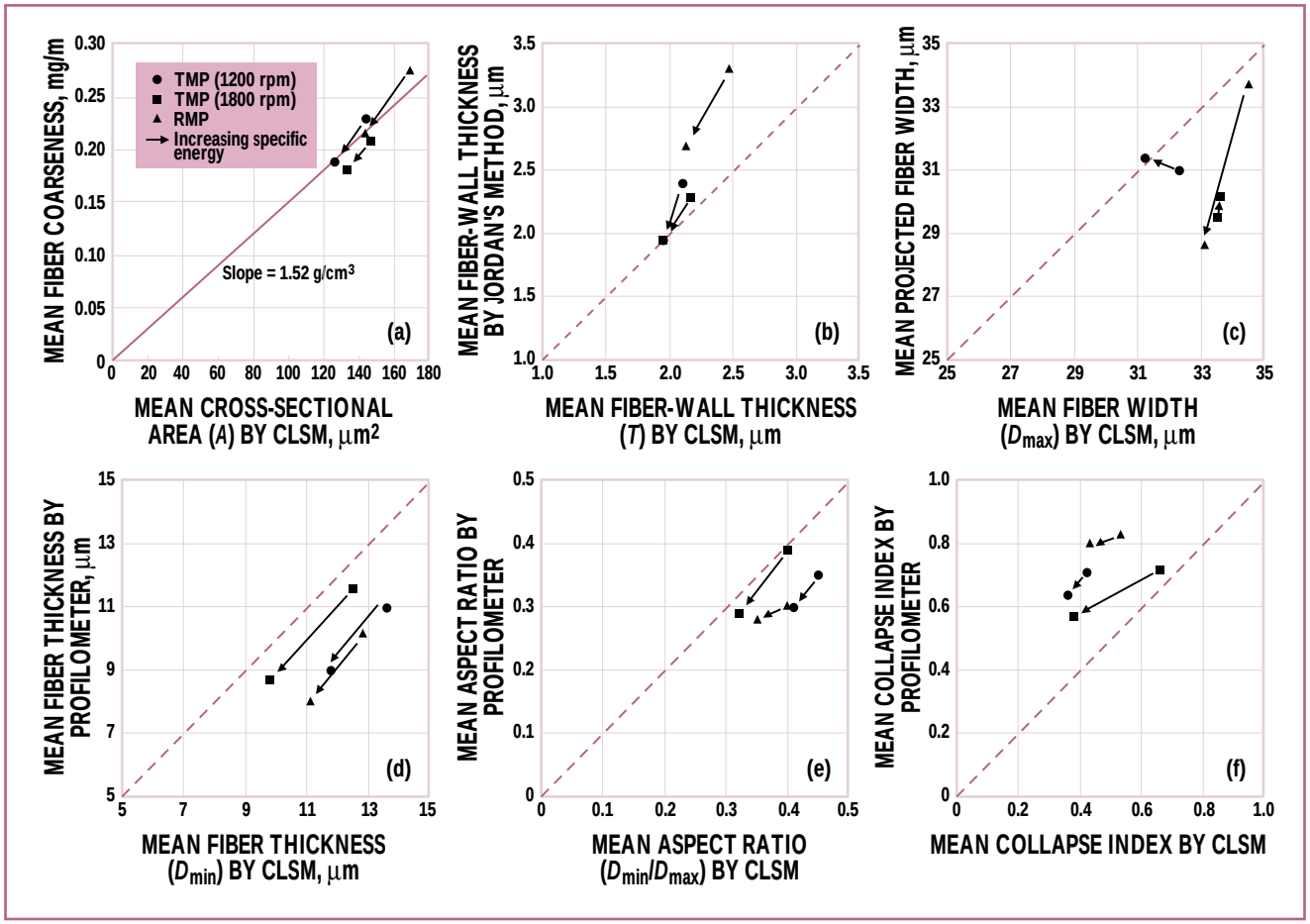

6. Comparison of fiber properties as measured by conventional techniques (y-axis) and CLSM (x-axis): (a) fiber coarseness (Clark method) vs. cross-sectional area; (b) wall thickness (Jordan's method) vs. wall thickness; (c) projected fiber width vs. D_{max}; (d) fiber thickness (profilometer) vs. D_{min}; (e) aspect ratio (profilometer) vs. aspect ratio; and (f) collapse index (profilometer) vs. collapse index. Arrows indicate changes in fiber property with increasing specific energy.

KEYWORDS

Collapse, cross section, dimensions, energy, fiber dimensions, fibers, intensity, lasers, mechanical pulps, microscopy, properties, pulps, refining sections.

changes in transverse fiber dimensions of mechanical pulp fibers produced under different refining conditions. The results show that increasing the specific energy of refining results in a decrease of mean fiber cross-sectional area, fiber-wall thickness, fiber thickness, lumen area, and aspect ratio. These effects become more pronounced with high-intensity refining. The decrease in fiber-wall thickness with increasing energy and intensity promotes fiber collapsibility. During high-intensity refining, fiber collapse appears to be further enhanced by a decrease in the rigidity of the fiber wall.

Measurements of fiber transverse dimensions obtained using conventional methods were in fair agreement with the results obtained using CLSM. However, the fiber cross-sectional images generated by CLSM provide a more reliable means of measuring any fiber transverse dimension. TJ

Jang is a scientist, Amiri is a research engineer, Seth heads the Fiber and Product Quality Section, and Karnis directs the Mechanical Pulping Division of the Pulp and Paper Research Institute of Canada, 3800 Wesbrook Mall, Vancouver, BC, Canada V6S 2L9.

The authors express their appreciation to V. Amarasinghe and B. K. Chan for generating CLSM images and conducting image analysis. The technical assistance of M. Grondin, J. Mathieu, and G. Stepien in measuring fiber properties is gratefully acknowledged. Special thanks are due to A. G. Robertson for helpful discussions.

Received for review Sept. 23, 1994.

Accepted June 30, 1995.

LITERATURE CITED

1. Miles, K. B., May, W. D., and Karnis, A., *Tappi J.* 74(3): 221(1991).
2. Stationwala, M. I., Miles, K. B., and Karnis, A., *J. Pulp Paper Sci.* 17(1): J12(1991).
3. Heikkurinen, A., Vaarasalo, J., and Karnis, A., *J. Pulp Paper Sci.* 19(3): J119(1993).
4. Miles, K. B., *Paperi Puu* 72(5): 508(1990).
5. Sundholm, J., Heikkurinen, A., and Mannstrom, B., *Paperi Puu* 70(5): 446(1988).
6. Karnis, A., *J. Pulp Paper Sci.* 20(10):J280 (1994).
7. Jang, H. F., Robertson, A. G., and Seth, R. S., *Tappi J.* 74(10): 217(1991).
8. Amiri, R., Görres, J., Grondin, M., *et al., Transactions of the Tenth Fundamental Research Symposium,* Mechanical Engineering Publications, London, 1993, p. 285.
9. Jang, H. F., Robertson, A. G., and Seth, R. S., *J. Matl. Sci.* 27: 6391(1992).
10. Kibblewhite, R. P. and Bawden, A. D., *Proceedings of PIRA Conference on Current and Future Technologies of Refining,* PIRA, Leatherhead, UK, Dec. 1991, paper 6.
11. Page, D. H., *Tappi* 50(9): 449(1967).
12. Jang, H. F. and Seth, R. S., to be submitted.
13. "Coarseness of pulp fibers," TAPPI Test Method T 234 cm-84, TAPPI PRESS, Atlanta.
14. Jordan, B. D., *J. Pulp Paper Sci.* 14(2): J44(1988).